

Coordination Studies of Al-EDTA in Aqueous Solution

Orkid Coskuner^{*,†,‡,§} and Emily A. A. Jarvis^{†,||}

Physical and Chemical Properties Division, National Institute of Standards and Technology, 100 Bureau Drive, Mail Stop 8380, Gaithersburg, Maryland 20889, and Synchrotron Radiation Laboratory, Stanford University, 2575 Sand Hill Road, Palo Alto, California 94025

Received: October 9, 2007; In Final Form: December 9, 2007

The degree of aluminum toxicity is based on its complexation with organic ligands. One of these complexes is AIEDTA⁻ (Al = aluminum, EDTA = ethylenediaminetetraacetate), the structure of which in aqueous solution has been debated on the basis of X-ray absorption and NMR measurements with different interpretations proposing different coordination. In addition, there is a lack of consensus regarding the relationship of crystalline AIEDTA⁻ and its geometry in solution. This debate must be resolved, not merely for scientific interest, but because the use of an incorrect coordination might lead to the wrong interpretation of bioactivity and kinetics data. In this work, we predict the coordination of Al in aqueous AIEDTA⁻ by employing ab initio calculations and Car–Parrinello molecular dynamics simulations. Our results indicate that AIEDTA⁻ favors Al in octahedral coordination in aqueous solution. Furthermore, the predicted crystalline and solution-phase structures of AIEDTA⁻ are similar and agree well with recent X-ray measurements, supporting the strong chelating nature of this metal–organic complex in aqueous solution.

I. Introduction

The impact of metal ions and their metal organic complexes is ubiquitous across such diverse fields as nanotechnology, environmental chemistry, catalysis, and medicine. The chemistry of metal organic complexes is extremely important for a wide range of environmental and biological processes that depend on metal ions as active participants.^{1–4} Organic complexes that contain metal ions as key components are becoming increasingly prevalent as diagnostic or therapeutic agents for treating a wide variety of metabolic disorders and diseases; for example, calcium disodium ethylenediaminetetraacetate [CaNa₂EDTA] is among the recent chelating drugs with worldwide application.⁵ Although certain metal complexes may prove valuable to human health, complexation of some metals with organic ligands also has the potential to increase the degree of their toxicity. Aluminum (Al) is known to be toxic to many organisms in soils and surface waters.^{6–9} In addition, Al is a well-known neurotoxin in humans,¹⁰ and is suspected to play a role in the pathogenicity of Alzheimer's disease.^{11,12} It has also been found in high concentrations in the hair of children with dyslexia and behavioral problems.^{13,14}

Studies have indicated that EDTA reduces the toxicity of Al to fish.¹⁵ In humans, complexation by organic ligands may enhance Al absorption in the digestive tract,¹⁶ but alternatively can be used as a means of removing Al from the human body, as with desferrioxamine treatments.¹⁷ Given the use of EDTA in chelation therapy,^{18,19} its use in solubilizing metals,²⁰ and its widespread use in industrial applications and subsequent pol-

lution risks,^{21,22} the impact of EDTA on Al transport and bioavailability is of significant importance.

Understanding the behavior of Al–EDTA complexes in environmental and biological systems requires detailed knowledge of molecular structure. The coordination of AIEDTA⁻ in crystalline solids is well established. X-ray crystallographic studies performed on (NH₄)[Al(EDTA)]·2H₂O and K[Al(EDTA)]·2H₂O show that AIEDTA⁻ forms an octahedral complex in the solid state.^{23,24} Its coordination in water is less clear, with conflicting interpretations arising based on spectroscopic measurements. Iyer et al. proposed a hexadentate binding for EDTA based on a comparison of the ²⁷Al–NMR chemical shifts of AIEDTA⁻ and other Al–aminocarboxylate complexes.²⁵ Recently, Jung et al. studied the structure of aqueous Al–EDTA by ¹³C and ¹H NMR spectroscopy and also proposed an octahedral, hexadentate structure for aqueous AIEDTA⁻, similar to that observed in the crystalline structure.²⁴ However, Matsuo et al. recently proposed a trigonal bipyramidal aqueous Al(H₂O)EDTA⁻ coordination based on X-ray absorption spectroscopic results and first-principles calculations.²⁶ This structure includes a water molecule in the Al coordination sphere and tetradentate ligation by EDTA, leaving two acetate groups uncoordinated. Unequivocal determination of the aqueous Al–EDTA structure is necessary to understand its chemical behavior. For example, Nemes et al.²⁸ assumed a seven-coordinated structure based on Fe–EDTA studies in interpreting their kinetic data for the formation of the [AIEDTAF]²⁻ complex, with the water ligand as the presumed leaving group; the interpretation of their kinetic data could be different if they assumed a different Al coordination for Al–EDTA.

Given the wide range of structural interpretations of experimental measurements in aqueous solution, theoretical studies can play an important role in determining the coordination chemistry and structure of metal ions and metal–organic species in water. In general, first-principles methods have been applied to study the interactions between various metal ions and organic

* Corresponding author. E-mail address: orkid.coskuner@nist.gov.

[†] National Institute of Standards and Technology.

[‡] Stanford University.

[§] Additional current address: Computational Materials Sciences Center, College of Science, George Mason University, Research I, Fairfax, Virginia 22030.

^{||} Current address: Gordon College, 255 Grapevine Road, Wenham, Massachusetts 01984.

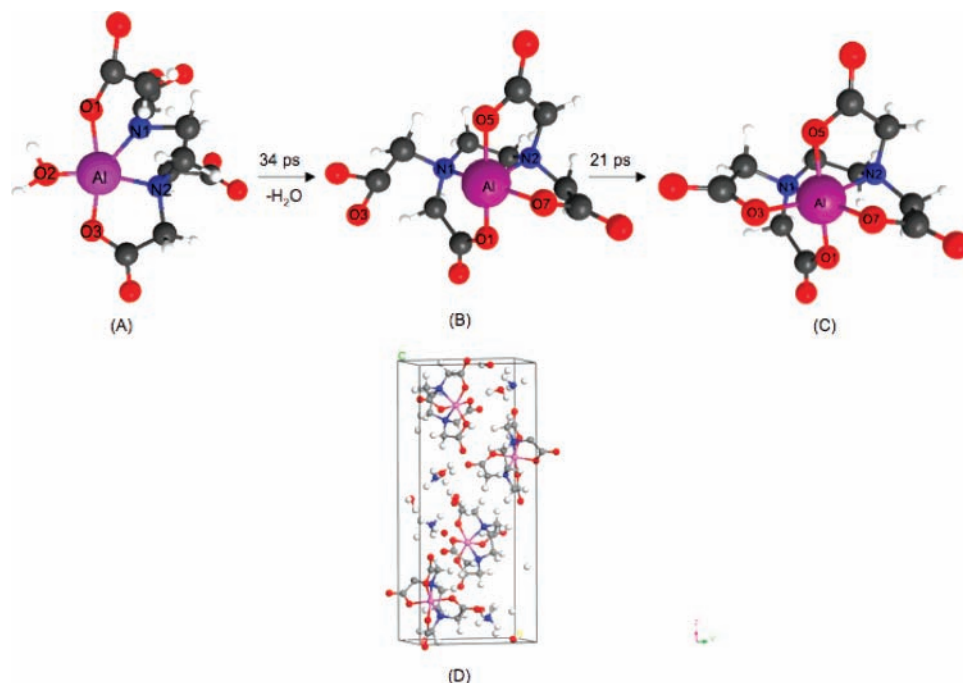


Figure 1. $\text{Al}(\text{H}_2\text{O})\text{EDTA}^-$ with two uncoordinated acetate groups (A), AlEDTA^- structure with one uncoordinated acetate group (B), and octahedral AlEDTA^- structure (C) obtained from CPMD simulations. (D) The optimized crystalline structure of the octahedral AlEDTA^- with its counterions in its environment utilizing the PBE method along with a DNP basis set (see Methods section for details).

molecules. An example is the recent work of Sillanpaa et al., who concluded using density functional theory that the complexation of polycarboxylic acids with calcium, manganese, iron, magnesium, and zinc ions depends strongly on the particular metal ion.²⁹ Furthermore, the interaction of the hydrated Al(III) ion with acetate ions was studied by Tunega et al., who employed various first-principles methods and proposed that Al–monodentate species are slightly more stable than Al–bidentate species.³⁰ In addition, Rezabal et al. investigated the properties of the coordination shell of Al(III) in a model protein environment with an acetate ligand attached to the metal ion using density functional theory.³¹ Their calculations showed that the presence of an acetate group promotes the formation of Al–organic complexes.

The conformation of a biomolecule in water is assumed to be determined by steric interactions and inter- and intramolecular hydrogen bonding. Static first-principles calculations in the gas phase and in a continuum environment of water, which are mentioned above, cannot capture the impact of both dynamics and intermolecular hydrogen bonding between the solute and surrounding water molecules on the metal–organic structure. Encouraged by recent successful *ab initio* molecular dynamics simulation investigations of metal ions and biological molecules in water,^{32,33,35} we studied the preferred geometry and conformation of Al–EDTA in water using explicit water molecules: the forces acting on the particles were obtained for each time step from first-principles electronic structure calculations by Car–Parrinello molecular dynamics (CPMD) simulations. For the static first-principles calculations in a continuum water environment, methods yielding hydration enthalpy values for Al(III) ion close to experimental data were chosen for determining the most likely Al coordination in aqueous AlEDTA^- . Results obtained from CPMD simulations using explicit water molecules were compared to those obtained from static first-principles calculations utilizing a continuum model for water. According to our studies, the aqueous octahedral AlEDTA^- structure is preferred over the aqueous trigonal bipyramidal

$\text{Al}(\text{H}_2\text{O})\text{EDTA}^-$ structure proposed by Matsuo et al.²⁶ In addition, we optimized the solid-state $\text{NH}_4(\text{AlEDTA})\cdot 2\text{H}_2\text{O}$ structure for comparison with the diffraction results of Jung et al.²⁴ This allowed us to assess the structural similarity of crystalline and aqueous AlEDTA^- , which has recently been debated on the basis of spectroscopic measurements.

II. Methods

1. CPMD Simulations. All CPMD simulations were performed using the NWCHEM program.^{34a} The initial configurations were taken from equilibrated classical MD simulations of Al–EDTA and 216 water molecules at 300 K and at a pressure of 0.1 MPa. The OPLS-AA, UFF, and modified TIP5P parameters were chosen for the classical simulations of EDTA, Al, and water, respectively.^{34b–d} Lorentz–Berthelot mixing rules were applied for calculating the cross-parameters.³⁷ The PBE functional for exchange–correlation was applied along with Troullier–Martin pseudopotentials.^{35,36} The electronic wave functions were expanded in a plane wave basis set with a kinetic energy cutoff of 110 Ry. A time step of 0.1 fs was employed in these simulations, the electronic mass was set to 900 a.u., and the isotopic mass of deuterium was used for hydrogen.

Simulations for 80 ps were performed, and the statistics were collected for the last 70 ps for the structural studies of recently proposed Al–EDTA species in water. Isothermal–isobaric ensemble CPMD simulations of each Al–EDTA species (Figure 1A–C) and 32 water molecules (first-shell water molecules; initial trajectory taken from classical MD simulations of Al–EDTA and 216 water molecules) were performed on trajectories obtained from classical MD simulations at 300 K and at a pressure of 0.1 MPa using a Nose–Hoover thermostat. Long-range interactions were treated with the Ewald sum method.³⁷

Encouraged by recently presented potential of mean force (PMF) calculations via CPMD simulations for biological molecules in water,³² the PMF for the coordination of the acetate

groups to the Al(III) ion was calculated using eq 1 to study the preferred coordination for Al-EDTA in water.

$$\Delta G = -kT \log Z \quad (1)$$

where Z is the probability of finding the acetate group coordinated to Al in water. In this work, a distance of 1.8 Å presents coordinated acetate groups and larger distances (up to 5.5 Å) present uncoordinated acetate groups. For the first set of PMF calculations, we defined the equilibrated Al(H₂O)EDTA⁻ structure (Figure 1A) taken from CPMD simulations as the initial state, and the AlEDTA⁻ structure with one uncoordinated acetate group (Figure 1B) that was obtained from our CPMD simulations as the final state. For the second set of PMF calculations (coordination of the second acetate group), we used the AlEDTA⁻ structure with one uncoordinated acetate group as the initial state, and the octahedral AlEDTA⁻ structure with the hexadentate ligation of EDTA (Figure 1C) that was obtained from our CPMD simulations as our final state. For these calculations ($\lambda = 0 \rightarrow \lambda = 1$, where $\lambda = 0$ and $\lambda = 1$ are the initial and final states), the system (Al-EDTA and 32 water molecules) was simulated for 60 ps for each window. To check the adequacy and the convergence of the computed PMF using 20 windows, we compared the PMF results for $\lambda = 0 \rightarrow \lambda = 1$ to those computed for $\lambda = 1 \rightarrow \lambda = 0$, and found that the PMFs exhibit the same profiles. We also calculated the PMFs from 30, 40, and 50 ps CPMD simulations for each window and determined the standard deviation in PMF arising from these different simulation times. Calculated standard deviation is between 0.2% and 4.1% for 50 and 60 ps simulations.

2. Ab Initio Calculations. Ab initio calculations were performed with the GAMESS program^{38,39} in the gas phase and in aqueous solution using a continuum model for water. No symmetry constraints were enforced during geometry optimization. Free energy values in aqueous solution computed by continuum models can be sensitive to the radius of the cavity surrounding the species embedded in the continuum. Klamt et al. optimized the van der Waals radii of carbon, oxygen, nitrogen, and hydrogen and implemented them in the COSMO program.^{40,41} The van der Waals radii for other elements are typically treated as default values within this program. In this work, we performed calculations in order to fit the van der Waals radius of the Al(III) ion to the experimental free energy value of -4619.1 kJ mol⁻¹.^{42,43} In these calculations, the van der Waals radius was fitted to the free energy as follows:

$$\Delta G[\text{Al(III)}] = \Delta G_{\text{water}}[\text{Al(III)}, r] - \Delta G_{\text{gas}}[\text{Al(III)}, r] \quad (2)$$

where r is the van der Waals radius of the Al(III) ion, $\Delta G_{\text{water}}[\text{Al(III)}, r]$ is the corrected energy for the Al(III) ion in COSMO water, and $\Delta G_{\text{gas}}[\text{Al(III)}, r]$ is the corresponding free energy in the gas phase. Our optimized van der Waals radius is 1.33 Å and is in agreement with the Al(III) radius recently presented by Saukkoriipi et al.⁴⁴ Our benchmark calculations indicate that the PBE method with the cc-pVTZ basis set, using the optimized van der Waals radius of 1.33 Å for the Al(III) ion with the COSMO program, effectively reproduces the experimental hydration enthalpy of the Al(III) ion (see Appendix). Accordingly, we studied the structural and thermodynamic properties of the aqueous Al-EDTA structures using the PBE/cc-pVTZ level of theory.

The crystalline structure of AlEDTA⁻ (Figure 1D) with its counterions was optimized for comparison with the detailed ionic coordinates that were measured by Jung et al.²⁴ We employed the experimental lattice vectors and optimized the

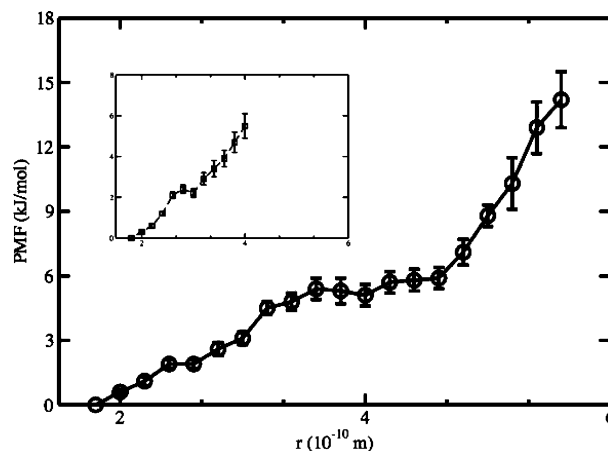


Figure 2. Calculated PMF values for the coordination of an acetate group on Al(III) in Al-EDTA. The distance $r(\text{O}-\text{Al}) = 5.5$ Å belongs to the uncoordinated acetate groups in Al(H₂O)EDTA⁻, and the distance $r(\text{O}-\text{Al}) = 1.8$ Å represents the coordinated acetate group in AlEDTA⁻. The inset plot presents the calculated PMF for the coordination of the second acetate group (see Methods section for details).

ionic coordinates without any symmetry constraints using periodic DFT with the PBE exchange-correlation functional and a DNP basis within the program DMOL.^{3,45,46} These calculations were performed using a $2 \times 3 \times 1$ \mathbf{k} -point mesh. PBE results obtained on AlEDTA⁻ using the Gaussian and numerical basis sets were not significantly different.

III. Results and Discussion

Figure 1 displays the mechanism for Al and EDTA coordination obtained from our CPMD simulations. These simulations provide insight into dynamical events that are difficult to observe experimentally. The initial Al(H₂O)EDTA⁻ structure with two uncoordinated acetate groups and one water molecule attached to Al, recently proposed by Matsuo et al. on the basis of XANES measurements, is shown in Figure 1A.²⁶ The 5-fold Al in AlEDTA⁻ with one uncoordinated acetate group is presented in Figure 1B. The octahedral AlEDTA⁻ with the hexadentate binding of EDTA, which was proposed by Jung et al. on the basis of X-ray and NMR spectroscopy measurements,²⁴ is illustrated in Figure 1C.

The initial trajectory that is used in our simulations belongs to Al(H₂O)EDTA⁻. We observe a larger distance between the coordinated water molecule and the Al(III) ion within 8 ps of simulations. This water molecule moves and leaves the Al(III) ion dehydrated in the following 11 ps. Once the water molecule coordinates to a first-shell water molecule through hydrogen bonding, the distance between the acetate group oxygen atoms and the Al(III) ion starts decreasing. The first acetate oxygen becomes attached to the Al(III) ion within the next 15 ps, forming an AlEDTA⁻ with one uncoordinated acetate group in water. In the following 21 ps simulations, the uncoordinated acetate group oxygen atom coordinates to the Al(III) ion, and the water molecule that was coordinated to Al in Al(H₂O)EDTA⁻ moves to the second shell. The octahedral AlEDTA⁻ structure stays octahedral for the rest of the simulation time. No return paths to the 5-fold Al in AlEDTA⁻ with one uncoordinated acetate group and to the Al(H₂O)EDTA⁻ structures have been observed.

Calculated PMF values based on the coordination of the acetate groups are presented in Figure 2. These results show that the coordination of acetate groups and the removal of a water molecule from the Al(III) coordination sphere stabilize the metal-organic complex in aqueous solution. According to

TABLE 1: Calculated NPAs for Al and for the Coordination Sphere Atoms of the Al-EDTA Species Using the PBE Method and cc-pVTZ Basis Set

octahedral AIEDTA ⁻		trigonal pyramidal Al(H ₂ O)EDTA ⁻		AIEDTA ⁻ with one uncoordinated acetate group	
Al	+1.86	Al	+2.01	Al	+1.93
N1	-0.55	N1	-0.65	N1	-0.60
N2	-0.55	N2	-0.64	N2	-0.59
O1	-0.79	O1	-0.83	O1	-0.81
O3	-0.80	O2 (water)	-1.03	O2	-0.83
O5	-0.79	O3	-0.87	O3 (uncoordinated)	-0.30
O7	-0.80				

our PMF calculations, the AIEDTA⁻ with one uncoordinated acetate group (Figure 1B) is preferred over the Al(H₂O)EDTA⁻ structure (Figure 1A). Furthermore, the coordination of the second acetate group to the Al(III) ion further stabilizes the complex in water: the octahedral AIEDTA⁻ structure (Figure 1C) is preferred over the AIEDTA⁻ structure with one uncoordinated acetate group (Figure 1B). Overall, these simulations demonstrate that the octahedral coordination of the AIEDTA⁻ complex that was proposed by Jung et al.²⁴ is preferred over the Al(H₂O)EDTA⁻ structure, which was presented by Matsuo et al.²⁶

In addition to the CPMD simulations, we also optimized the structures of the octahedral AIEDTA⁻ and trigonal pyramidal Al(H₂O)EDTA⁻ and calculated their Gibbs free energies at room temperature with the PBE/cc-pVTZ method using a continuum model for water (see Methods section). According to these studies, the octahedral AIEDTA⁻ structure (Figure 1C) is preferred over the Al(H₂O)EDTA⁻ structure (Figure 1A) by 9.6 kJ mol⁻¹. These findings illustrate that the thermodynamic trend obtained from static DFT calculations in a continuum water environment agrees with that obtained via CPMD simulations using explicit water molecules (see above) for this metal–organic complex.

These findings also suggest that the type of ligand attached to the metal ion, i.e., Lewis-base strength, is the key factor in determining the coordination of a metal–organic complex, with acetate being a better Lewis base than a water molecule. The results described above support the theoretical studies of Rezaal et al.,³¹ who concluded that the presence of an acetate group promotes the formation of Al–acetate species. Furthermore, our thermodynamic studies, which present the octahedral AIEDTA⁻ as the preferred coordination, are in agreement with the experimental studies of Jung et al.,²⁴ who proposed an octahedral AIEDTA⁻ geometry in aqueous solution.

The optimization of the Al(H₂O)EDTA⁻ structure in a continuum water environment, using the PBE method with the cc-pVTZ basis set, led to two local minima structures: pyramidal and trigonal bipyramidal geometries. The calculated Gibbs free energies for both structures in a continuum water environment show that the trigonal bipyramidal is preferred over pyramidal Al(H₂O)EDTA⁻ structure by 4.5 kJ mol⁻¹. This finding supports the observations of Matsuo et al., who reported aqueous pyramidal and trigonal bipyramidal structures in 4:6 proportion on the basis of NMR measurements.²⁶ No pyramidal structure was obtained from our CPMD simulations for Al(H₂O)EDTA⁻ utilizing explicit water molecules.

Natural partial charge analysis (NPA) for the optimized octahedral AIEDTA⁻ and Al(H₂O)EDTA⁻ structures using a continuum model for water, described above, are listed in Table 1. Although the metal center possesses a formal oxidation state of +3, the partial charges determined using the NPA analysis are lower, indicative of the electron density donation from the

TABLE 2: Specific Optimized Bond Lengths and Angles of the Octahedral AIEDTA⁻ Complex (Figure 1C) Calculated in Aqueous Solution and in the Solid State with the Static PBE Method Using DNP and cc-pVTZ Basis Sets, and a Comparison to Results Obtained from CPMD Simulations^a

	CPMD			
	simulations aqueous phase	PBE/cc-pVTZ aqueous phase	PBE/DNP crystalline	experimental crystalline
Al–N1/Å	2.07 ± 0.03	2.09	2.08	2.07
Al–N2/Å	2.03 ± 0.05	2.09	2.05	2.05
Al–O1/Å	1.85 ± 0.03	1.91	1.89	1.88
Al–O3/Å	1.86 ± 0.05	1.88	1.90	1.87
Al–O5/Å	1.85 ± 0.05	1.92	1.92	1.88
Al–O7/Å	1.87 ± 0.04	1.88	1.89	1.85
N1–Al–O1/deg	84.8 ± 3.4	83.5	84.4	83.7
N2–Al–O1/deg	86.3 ± 4.1	93.2	95.3	94.0
N1–Al–O3/deg	85.2 ± 2.9	83.4	83.4	83.2
N1–Al–O5/deg	89.3 ± 4.5	93.1	93.6	92.4
N1–Al–N2/deg	85.8 ± 2.7	84.9	86.0	84.8
N2–Al–O5/deg	84.2 ± 3.3	83.5	83.8	83.7
N2–Al–O7/deg	85.6 ± 4.0	83.3	83.5	83.3
O1–Al–O3/deg	92.7 ± 3.6	94.8	94.0	93.8
O3–Al–O5/deg	88.9 ± 3.9	87.8	86.5	87.6
O1–Al–O5/deg	176.2 ± 2.8	175.5	177.9	175.6
O1–Al–O7/deg	90.1 ± 3.3	87.8	87.7	88.0

^a The experimental values listed were obtained by Jung et al.³⁴ using X-ray diffraction. Atom numbers listed here are illustrated in Figure 1C.

ligands to the metal center. We note the larger partial positive charge on Al in Al(H₂O)EDTA⁻ relative to the partial charge value calculated for Al in the octahedral AIEDTA⁻ structure. This result indicates that the partial positive charge on Al decreases with increasing ratio of bonding CH₂COO groups. Furthermore, the replacement of the water molecule by an acetate group increases the donation of electron density from the ligand to the metal ion. These findings support the better Lewis base character of an acetate ligand.

The debate about the preferred coordination of Al–EDTA in aqueous solution has sparked the question of how the aqueous solution structure of Al–EDTA relates to its crystalline structure. Our DFT calculation as well as CPMD simulation results show that the preferred octahedral AIEDTA⁻ structure in water does not deviate more than 3–4% from its theoretically optimized and experimentally proposed solid-state structures (Table 2). The ring strain methodology, which was defined by Weakliem and Howarth for solid-state structures, was applied.⁴⁷ According to this terminology, the N1–Al–O1 (Figure 1C) five-membered ring is defined as *R*, and N1–Al–O3 as well as N2–Al–O7 are called *G* rings. The five-membered ring with the two nitrogen atoms, aluminum, and the two methylene carbon atoms is designated as *E* (Figure 1C). The *E* ring is supposed to have an ideal angle sum of 538.9° according to this methodology.⁴⁷ The calculated angle sum values of *R*, *G*, and *E* rings for the optimized crystal structure (Figure 1D) and for the octahedral AIEDTA⁻ complex in water, using ab initio methods, CPMD simulations, and their comparison to experimental values, are given in Table 3. According to these values, the *E* ring is the highest strained ring of the octahedral AIEDTA⁻ in both solid state and in water, while the two *R* rings present relaxed rings in both phases. Moreover, the results in water show a deviation of 2–6% from the experimental angle sum values measured by Jung et al., who employed X-ray diffraction.²⁴ Our studies indicate that both the implicit and explicit solvent models provide consistent ring strain trends for the octahedral AIEDTA⁻ complex.

TABLE 3: Calculated Angle Sums for the *E*, *R*, and *G* Rings of the Octahedral AIEDTA[−] Structure Employing CPMD Simulations Using Explicit Water Molecules, Static PBE Calculations with the cc-pVTZ Basis Set Utilizing a Continuum Model for Water at Room Temperature and Their Comparison to the Angle Sums Obtained for the Octahedral AIEDTA[−] Structure in the Solid State with the PBE Method Utilizing a DNP Basis Set, and the Ring Angle Sums Based on the X-ray Diffraction Measurements by Jung et al.

ring	PBE/cc-pVTZ	CPMD		experimental solid state
	in water (COSMO)	simulations in water	PBE/DNP solid state	
<i>G</i> (O3, N1 chelation)	526.2	523.8 ± 5.2	527.2	526.8
<i>G</i> (O7, N2 chelation)	525.4	522.1 ± 4.8	523.7	524.5
<i>R</i> (N2, O5 chelation)	538.1	535.4 ± 5.2	537.5	537.1
<i>R</i> (N1, O1 chelation)	538.4	540.7 ± 3.8	538.2	538.2
<i>E</i>	516.0	518.8 ± 3.4	515.9	515.7

IV. Conclusion

We have used ab initio calculations and CPMD simulations to identify the recently debated structure of the Al–EDTA complex in aqueous solution. The insights obtained from the simulations lend additional support to some previous experimental studies, and prove to be valuable in interpreting previously performed spectroscopy measurements.

Our PMF calculations utilizing CPMD simulations and Gibbs free energy calculations using static DFT calculations suggest a hexadentate coordination for Al in AIEDTA[−] in water and show agreement with the studies of Jung et al.,³⁴ who performed X-ray measurements on the solid structure and NMR spectroscopy on the aqueous AIEDTA[−] complex. Furthermore, our NPA analyses reveal that the coordination of an acetate group donates more electron density to the metal ion relative to a water molecule, which may indicate the superior Lewis base characteristics of an acetate over a water molecule as a ligand.

Another key finding from the calculations is the structural similarity of the octahedral AIEDTA[−] in aqueous solution and in the solid state. These findings suggest that the crystalline structure of octahedral AIEDTA[−] does not change significantly in aqueous solution, whether utilizing implicit or explicit models for water. In addition, our optimized structure for the solid-state octahedral AIEDTA[−] agrees well with earlier X-ray measurements of the crystalline AIEDTA[−].

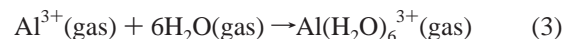
This study presents the first ab initio molecular dynamics simulations using the Car–Parrinello method of Al–EDTA species in aqueous solution. Structural and thermodynamic results for AIEDTA[−] that are presented and discussed herein, determined by CPMD simulations utilizing explicit water molecules and static DFT using a continuum model for water, show similar predictions, indicating neither the dynamics nor intermolecular hydrogen bonding between the complex and surrounding water molecules significantly affect the stable octahedral AIEDTA[−] structure. We have demonstrated that the theoretical studies performed with an appropriate level of theory can provide complementary insights into the structural studies of metal–organic complexes in aqueous solution. Such simulations at the electronic level coupled with spectroscopic measurements can help to distinguish between competing metal–organic structures and verify experimental interpretations.

Acknowledgment. We thank T. C. Allison, M. Hay, S. Myneni, M. Gilson, C. Lo, and C. Gonzalez for helpful discussions. This study was supported by National Science Foundation Grant CHE-0431425 (Stanford Environmental Molecular Sciences Institute). E.A.A.J. acknowledges the National

Research Council and the National Institute Standards and Technology for an NRC-NIST Postdoctoral Fellowship. Certain commercial equipment and software are identified in this paper in order to specify the experimental procedure adequately. Such identification is not intended to imply recommendation or endorsement by the National Institute of Standards and Technology, nor is it intended to imply that the software or equipment identified are necessarily the best available for the purpose.

Appendix

The first part of our benchmark calculations focused on the calculations that were carried out for the isolated molecule in the gas phase. The formation energy in the gas phase, $\Delta E_f(\text{gas})$, was determined according to the following reaction:



Calculated $\Delta E_f(\text{gas})$ values obtained with various first-principles methods using the cc-pVTZ basis set are displayed in Table 4. Our optimized geometries and $\Delta E_f(\text{gas})$ value obtained with the MP2/cc-pVTZ method are in agreement with the MP2 results of Wassermann et al.⁴⁸ A comparison of formation energies shows that the HF result deviates stronger from both the MP2 and the PBE results. According to our results, the optimized geometries are relatively insensitive with respect to the basis set, but the computed $\Delta E_f(\text{gas})$ value depends on the basis set, which was also reported by Tunega et al.⁴⁹ and is presented in detail below.

TABLE 4: Computed Thermodynamic Properties of Al(H₂O)₆³⁺ in the Gas Phase and in Continuum Water Environment at 298.15 K Employing the PBE Method with the cc-pVTZ Basis Set

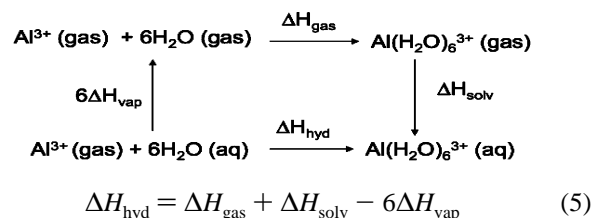
property/kJ mol ^{−1}	gas phase	aqueous phase
$\Delta E_o = \Delta E_f + \Delta E_{\text{ZPE}}^a$	−2861.7	−4639.7
$\Delta E_{298.15}$	−2886.8	−4655.2
ΔH	−2903.5	−4671.8

^a Here, ZPE denotes zero point energy.

The following thermodynamic approximation was used to calculate the enthalpy in the gas phase:

$$\Delta H_{\text{gas}} = \Delta E_f + \Delta E_{\text{ZPE}} + \Delta c_v T + \Delta(RT) \quad (4)$$

where ΔE_{ZPE} is the zero-point energy correction, $\Delta c_v T$ is the heat capacity contribution, and $\Delta(RT)$ represents the work term. Experimental gas-phase enthalpies are not available for comparison, but the standard hydration enthalpy in aqueous solution has been determined using calorimetric measurements. To calculate the hydration enthalpy for the Al(H₂O)₆³⁺ ion, we used the Born–Haber cycle presented in eq 5, similar to the approach utilized by Akesson et al. and Tunega et al.^{49–52}



The calculated thermodynamic values at the PBE/cc-pVTZ levels of theory for the Al(H₂O)₆³⁺ ion in the gas and aqueous phases are presented in Table 4. Our calculated solvation energy for water, which is necessary to determine the hydration enthalpy

of the $\text{Al}(\text{H}_2\text{O})_6^{3+}$ ion is -38.5 and -37.9 kJ mol^{-1} at the PBE/cc-pVTZ and MP2/cc-pVTZ levels of theory, respectively. These values are slightly higher than the experimental value⁵³ of -44.1 kJ mol^{-1} , but are in better agreement than the value of -28.6 kJ mol^{-1} reported by Tunega et al.⁴⁹ based on BLYP/SVP calculations using the PCM model for water. The experimental hydration enthalpy of $\text{Al}(\text{H}_2\text{O})_6^{3+}$ is -4668.3 ± 8.4 kJ mol^{-1} and agrees well with our PBE/cc-pVTZ calculated value of -4671.8 kJ/mol using eq 5.⁵⁴ Our calculations with the MP2/cc-pVTZ method predict a lower hydration enthalpy by 21.9 kJ mol^{-1} , whereas the hydration enthalpy we obtained from the HF calculations with the same basis set is 60.8 kJ mol^{-1} higher than the experimental value. The results obtained with the cc-pVDZ and 6-311 g(d+p) basis sets with the PBE exchange correlation functional yield 4–6% higher hydration enthalpies than the value obtained using the PBE/cc-pVTZ method and show larger deviations from the experimental value. Furthermore, the usage of the experimental hydration enthalpy for water (-41.7 kJ mol^{-1}) instead of our computed value for this property yields a hydration enthalpy for $\text{Al}(\text{H}_2\text{O})_6^{3+}$ that deviates 0.2% from our computed value that is presented above.

References and Notes

- (1) Karlin, K. D. *Science* **1993**, *261*, 701.
- (2) O'Halloran, T. V. *Science* **1993**, *261*, 715.
- (3) Finney, L. A.; O'Halloran, T. V. *Science* **2003**, *300*, 931.
- (4) Thompson, K. H.; Orvig, C. *Science* **2003**, *300*, 936.
- (5) Aposhian, H. V.; Aposhian, M. M. *Annu. Rev. Pharmacol. Toxicol.* **1990**, *30*, 279.
- (6) Foy, C. D.; Chaney, R. L.; White, M. C. *Annu. Rev. Plant Phys. Plant Mol. Biol.* **1978**, *29*, 511.
- (7) Kochian, L. V. *Annu. Rev. Plant Phys. Plant Mol. Biol.* **1995**, *46*, 237.
- (8) Burrows, W. D.; Hem, J. D. *CRC Crit. Rev. Environ. Control* **1977**, *7*, 167.
- (9) Gensemer, R. W.; Playle, R. C. *Crit. Rev. Environ. Sci. Technol.* **1999**, *29*, 315.
- (10) Kerr, D. N. S.; Ward, M. K.; Ellis, H. A.; Simpson, W.; Parkinson, I. S. Aluminum intoxication in renal disease. In *Aluminum in Biology and Medicine*; Ciba Foundation Symposium 169; John Wiley & Sons: Chichester, U.K., 1992.
- (11) Gauthier, E.; Fortier, I.; Courchesne, F.; Pepin, P.; Mortimer, J.; Gauvreau, D. *Environ. Res.* **2000**, *84*, 232.
- (12) Gupta, V. B.; Anitha, S.; Hegde, M. L.; Zecca, L.; Garruto, R. M.; Ravid, R.; Shankar, S. K.; Stein, R.; Shanmugavelu, P.; Rao, K. S. *J. Cell. Mol. Life Sci.* **2005**, *62*, 143.
- (13) Capel, I.; Pinnock, M.; Dorrell, H.; Williams, D.; Grant, E. *Clin. Chem.* **1981**, *6*, 879.
- (14) Marlowe, M.; Cossairt, A.; Moon, C.; Errera, J.; MacNeel, A.; Peak, R. *J. Abnorm. Child Psychol.* **1985**, *13*, 185.
- (15) Muramoto, S. *Bull. Environ. Contam. Toxicol.* **1981**, *27*, 221.
- (16) Martin, R. B. Aluminum speciation in biology. In *Aluminum in Biology and Medicine*; Ciba Foundation Symposium 169; John Wiley & Sons: Chichester, U.K., 1992.
- (17) Yokel, R. A. *Coord. Chem. Rev.* **2002**, *228*, 97.
- (18) Aposhian, H. V.; Aposhian, M. M. *Annu. Rev. Pharmacol. Toxicol.* **1990**, *30*, 279.
- (19) Waters, R. S.; Bryden, N. A.; Patterson, K. Y.; Veillon, C.; Anderson, R. A. *Biol. Trace Elem. Res.* **2001**, *83*, 207.
- (20) Jiang, X. J.; Luo, Y. M.; Zhao, Q. G.; Baker, A. J. M.; Christie, P.; Wong, M. H. *Chemosphere* **2003**, *50*, 813.
- (21) Bucheli-Witschel, M.; Egli, T. *FEMS Microbiol. Rev.* **2001**, *25*, 69.
- (22) Jones, P. W.; Williams, D. R. *Inorg. Chim. Acta* **2002**, *339*, 41.
- (23) Polynova, T. N.; Zasurskaya, L. A.; Ilyukhin, A. B. *Crystallogr. Rep.* **1997**, *42*, 155.
- (24) Jung, W. S.; Chung, Y. K.; Shin, D. M.; Kim, S. D. *Bull. Chem. Soc. Japan* **2002**, *75*, 1263.
- (25) Iyer, R. K.; Karweer, S. B.; Jain, V. K. *Mag. Res. Chem.* **1989**, *27*, 328.
- (26) Matsuo, S.; Shirozu, K.; Tateishi, Y.; Wakita, H.; Yokoyama, T. *Adv. Quantum Chem.* **2003**, *42*, 407.
- (27) Yokoyama, T.; Kurisaki, T.; Kinoshita, S.; Matsuo, S.; Wakita, H. *Anal. Sci.* **2000**, *16*, 647.
- (28) Nemes, J.; Tóth, I.; Zékány, L. *J. Chem. Soc., Dalton Trans.* **1998**, 2707.
- (29) Silanpaa, A. J.; Aksela, R.; Laasonen, K. *Phys. Chem. Chem. Phys.* **2003**, *5*, 3382.
- (30) Tunega, D.; Haberhauer, G.; Gerzabek, M.; Lischka, H. *J. Phys. Chem. A* **2000**, *104*, 6824.
- (31) Rezabal, E.; Mercera, J. M.; Lopez, X.; Ugalde, J. M. *J. Inorg. Chem.* **2006**, *100*, 374.
- (32) Coskuner, O. *J. Chem. Phys.* **2007**, *127*, 015101.
- (33) Coskuner, O. *J. Chem. Phys.* Submitted for publication, 2008.
- (34) (a) Bylaska, E.; de Jong, W. A.; Kowalski, K. *NWCHEM: A Computational Chemistry Package for Parallel Computers*, version 5.0; Pacific Northwest National Laboratory: Richland, Washington, 2006. (b) Damm, W.; Frontera, A.; Tirado-Rives, J.; Jorgensen, W. L. *J. Comput. Chem.* **1977**, *18*, 1955. (c) Rappe, A. K.; Casewit, C. J.; Colwell, K. S.; Goddard, W. A., III; Skiff, W. M. *J. Am. Chem. Soc.* **1992**, *114*, 10024. (d) Coskuner, O.; Deiters, U. K. *Z. Phys. Chem.* **2006**, *220*, 349.
- (35) Coskuner, O.; Jarvis, E. A. A.; Allison, T. C. *Angew. Chem., Int. Ed.* **2007**, *46* (41), 7853; *Angew. Chem.* **2007**, *119* (41), 7999.
- (36) Swaddle, T.; Rosenqvist, J.; Yu, P.; Bylaska, E.; Phillips, B.; Casey, W. H. *Science* **2005**, *308*, 1450.
- (37) Allen, M. P.; Tildesley, D. *Computer Simulations of Liquids*; Oxford University Press: New York, 1987.
- (38) Schmidt, M. W.; Baldrige, K. K.; Boatz, J. A.; Elbert, S. T.; Gordon, M. S.; Jensen, J. H.; Koseki, S.; Matsunaga, N.; Nguyen, K. A.; Su, S. J.; Windus, T. L.; Dupuis, M.; Montgomery, J. A. *J. Comput. Chem.* **1993**, *14*, 1347.
- (39) Gordon, M. S.; Schmidt, M. W. *Theory and Applications of Computational Chemistry*; Elsevier: Amsterdam, 2005.
- (40) Eckert, F.; Klamt, A. *Ind. Eng. Chem. Res.* **2001**, *40*, 2371.
- (41) Klamt, A.; Jonas, V. *J. Chem. Phys.* **1996**, *105*, 9972.
- (42) Burgess, J. *Metal Ions in Solution*; John Wiley & Sons: Chichester, U.K., 1978; p 186.
- (43) Tissandrier, M. D.; Cowen, K. A.; Femg, W. Y.; Gundlach, E.; Cohen, M. H.; Earhart, A. D.; Coe, J. V.; Tuttle, T. R., Jr. *J. Phys. Chem. A* **1998**, *102*, 7787.
- (44) Saukkoriipi, J.; Sillanpaa, A.; Laasonen, K. *Phys. Chem. Chem. Phys.* **2005**, *22*, 3785.
- (45) Delley, B. *J. Chem. Phys.* **1990**, *92*, 508.
- (46) Delley, B. *J. Chem. Phys.* **2000**, *113*, 7756.
- (47) Weakliem, A.; Howarth, J. L. *J. Am. Chem. Soc.* **1959**, *81*, 549.
- (48) Wassermann, E.; Rustad, J. R.; Xantheas, S. S. *J. Chem. Phys.* **1997**, *106*, 9769.
- (49) Tunega, D.; Haberhauer, G.; Gerzabek, M.; Lischka, H. *J. Phys. Chem. A* **2000**, *104*, 6824.
- (50) Akesson, R.; Petterson, L. M.; Sandstrom, G.; Wahlgreen, U. *J. Am. Chem. Soc.* **1994**, *116*, 8691.
- (51) Akesson, R.; Petterson, L. M. G.; Sandstrom, M.; Siegbahn, P. E.; Wahlgreen, U. *J. Phys. Chem.* **1992**, *96*, 10773.
- (52) Akesson, R.; Petterson, L. M. G.; Sandstrom, M.; Wahlgreen, U. *J. Am. Chem. Soc.* **1994**, *116*, 8705.
- (53) Franks, F. *Water: A Comprehensive Treatment*; Plenum Press: New York, 1975.
- (54) Smith, D. W. *J. Chem. Edu.* **1977**, *54*, 540.